Universal reaction-limited colloid aggregation

M. Y. Lin*
Department of Physics, Princeton University, Princeton, New Jersey 08544

H. M. Lindsay
Department of Physics, Emory University, Atlanta, Georgia 30322

D. A. Weitz
Exxon Research & Engineering Co., Route 22E, Annandale, New Jersey 08801

R. C. Ball
The Cavendish Laboratory, Madingly Road, Cambridge CB3 9HE England

R. Klein
Fakultät für Physik, Universitat Konstanz, Konstanz, West Germany

P. Meakin
E. I. du Pont de Nemours & Co., Experimental Station, Wilmington, Delaware 19880-0356
(Received 5 September 1989)

We study slow, or reaction-limited, colloid aggregation (RLCA) with both static and dynamic light scattering and develop a self-consistent interpretation of the results. Static light scattering is used to determine the fractal dimension of the clusters and the cutoff mass of the power-law cluster-mass distribution. Using this same cutoff cluster mass, we can predict the shape of the temporal autocorrelation function measured by dynamic light scattering. Good agreement with experiments is obtained provided the effects of rotational diffusion are included. In addition, we determine the ratio of the hydrodynamic radius to the radius of gyration of individual RLCA clusters and find $\beta=1.0$. A scaling method is used for the q-dependent first cumulants of the temporal autocorrelation functions to obtain a single master curve for data obtained at different times in the aggregation process. The shape of this master curve is very sensitive to several key features of the process of reaction-limited colloid aggregation. It allows us to unambiguously determine the exponent for the power-law cluster-mass distribution, $\tau=1.5\pm0.05$. Furthermore, we show that the master curves for three completely different colloids, gold, silica, and polystyrene, are indistinguishable. In addition, the fractal dimensions of their RLCA clusters, as measured by static light scattering, are all $d_f=2.1\pm0.05$, while the aggregation kinetics for each colloid are exponential. This demonstrates that reaction-limited colloid aggregation is universal, independent of the detailed chemical nature of the colloid system.

I. INTRODUCTION

Significant advances in our understanding of irreversible, kinetic colloid aggregation have been made in the past several years.[1-3] The structure of the colloidal aggregates has been shown to be scale invariant,[4] so that it can be characterized as a fractal, allowing a more detailed study of the process of aggregation and the relationship of the cluster structure to the aggregation kinetics. Two limiting regimes of kinetics have been identified: rapid, diffusion-limited (DLCA) and slow, reaction-limited (RLCA) colloid aggregation. Each regime exhibits distinct behavior, characterized by the fractal dimension of the clusters, the shape of the cluster mass distribution, and the kinetics of aggregation. This behavior is universal in that it is independent of the detailed nature of the colloid, provided the essential physical interactions are the same.[5,6] Furthermore, these two classes of aggregation are limiting regimes of the kinetics, both rapid and slow, and intermediate regimes of aggregation can often be described by a crossover behavior between the two limits. This suggests that DLCA and RLCA may be sufficient to describe the full range of kinetic aggregation.

In this paper, we present the results of a detailed study of the universal features of reaction-limited colloid aggregation. Our emphasis is on static and dynamic light scattering from the aggregating clusters, as these are particularly useful experimental probes of a colloid aggregation. Static light scattering probes the cluster structure, providing a measure of the fractal dimension. Dynamic light scattering probes the aggregation kinetics and is sensitive to the cluster mass distribution and its evolution in time as the aggregation proceeds.

Here, we show that the two types of scattering data can be interpreted self-consistently to obtain information about the structure of the colloidal aggregates and the

shape of the cluster mass distribution. We also show that all the dynamic light scattering data obtained while the aggregation proceeds can be scaled onto a single master curve. The shape of this curve is highly sensitive to several features of the aggregation process: the structure of the colloidal aggregates, including the anisotropy, and the shape of the cluster-mass distribution. Thus comparison of the master curves obtained from different colloids provides a critical test of the universality of the aggregation process.

We study the reaction-limited aggregation of three completely different colloids: gold, silica, and polystyrene. Using static light scattering, we show that the aggregates produced by each colloid have identical fractal dimensions $d_f = 2.1 \pm 0.05$. We obtain scaled master curves independently from the dynamic light scattering data for each of the colloids, and show that they are indistinguishable. The theoretical calculation of the shape of the master curves is shown to be in excellent agreement with the data, and allows us to determine the exponent for the power-law cluster mass distribution as $\tau = 1.5$ for all three colloids. Finally, we also show that the average cluster size for RLCA increases exponentially with time for all three colloids. From the identical behavior exhibited by these three completely different colloids, we conclude that reaction-limited colloid aggregation is universal.

In this paper, we restrict our attention to the regime of reaction-limited colloid aggregation. In this regime, the aggregation rate is very slow, making it easily accessible to light scattering experiments, and so fairly widely studied. In RLCA, the cluster-mass distribution has a power-law dependence on mass M, up to a cutoff mass M_c, $N(M) \sim M^{-\tau} \exp(-M/M_c)$. This power-law shape results in a subtle dependence of the dynamic light scattering data on the scattering wave vector, which is easily misinterpreted. This has lead to a range of reported values of τ in the literature. Thus, here we present a complete discussion of the behavior of dynamic light scattering and show that a correct treatment must include the proper evaluation of the consequences of the power-law shape of the cluster-mass distribution as well as the effects of the contribution of the rotational diffusion. When this is properly done, we show that it is possible to unambiguously determine the value of the cluster-mass exponent τ.

The rest of the paper is organized as follows. We first present a brief review of RLCA in Sec. II. In Sec. III, we describe the experimental details of the preparation of the colloids, their aggregation under reaction-limited conditions and the light scattering measurements. We then discuss in Sec. IV the results of both static and dynamic light scattering performed concurrently on the same sample and present a self-consistent interpretation of the data. In Sec. V, we discuss the calculation of the shape of the scaled master curve for the first cumulants of the autocorrelation functions measured with dynamic light scattering. We illustrate the pitfalls in the interpretation that can arise if the shape of the cluster-mass distribution and the effects of rotational diffusion are not properly included, and we discuss the correct interpretation. We then present the experimental determination of the master curve. In Sec. VI, we compare the experimentally measured master curves for the three completely different colloids and show that they are identical, demonstrating the universality of the RLCA regime. Finally, in Sec. VII we discuss other studies of RLCA, and resolve some discrepancies with the results reported here. A short conclusion closes the paper.

II. REACTION-LIMITED COLLOID AGGREGATION

A key to the understanding of all colloid aggregation is the behavior of the energy of interaction between two approaching particles.[7] For charge stabilized colloids, this can be understood within the Derjaguin-Landau-Verwey-Overbeek (DLVO) model, but the essential features are common to a much wider variety of colloids. The key feature is the repulsive energy barrier between two approaching colloidal particles. If the height of this energy barrier E_b is sufficiently large compared to $k_B T$, the particles will be unable to stick to one another when their diffusive motion causes them to collide, and the colloid will be stable against aggregation. Aggregation can occur only when the height of the barrier is reduced. If E_b is reduced to much less than $k_B T$, every collision will result in the particles sticking together, leading to very rapid aggregation, limited only by the rate of diffusion-induced collisions between the clusters. This regime is therefore called diffusion-limited colloid aggregation. By contrast, if E_b remains comparable to, or larger than, $k_B T$, many collisions must occur before two particles can stick to one another. In this case, the aggregation rate is limited by the probability of overcoming the repulsive barrier $P \sim \exp(-E_b/k_B T)$, leading to much slower aggregation. This regime is therefore called reaction-limited colloid aggregation. In each case, however, as particles stick together to become clusters, the clusters themselves continue to diffuse, collide, and aggregate. Thus both regimes are examples of cluster-cluster aggregation. Furthermore, in either case, the strength of the resultant bonds are much larger than $k_B T$, so the aggregation is irreversible and the clusters formed are rigid.

The qualitative behavior of the reaction-limited regime can be understood in simple terms.[8] Since $P \ll 1$, numerous contacts are required before two clusters stick together, resulting a very slow rate of aggregation. As the aggregation progresses, clusters with different masses are formed, as first single particles and then clusters stick to one another. However, since the sticking probability of two clusters is proportional to both P and to the number of available bonding sites, clusters with larger mass, and hence more potential bonding sites, grow faster than the smaller ones. These growth kinetics always leave a large number of small clusters behind, resulting in a highly polydisperse cluster mass distribution. By the same token, while the initial aggregation rate is very slow because all the clusters are small, the rate increases as the characteristic cluster size grows. In fact, the average cluster size increases exponentially in time. The growth kinetics as well as the cluster-mass distribution will in

turn influence the structure of the clusters formed. Since the sticking probability is very low, two approaching clusters can, on a statistical basis, sample all possible mutual configurations before they finally stick together. Thus the smaller clusters in the polydisperse distribution have a high probability of interpenetrating the large ones. In addition, the polydispersity of the cluster-mass distribution results in many collisions involving clusters of very different masses. These two effects lead to less tenuous clusters with a resultant increase in the fractal dimension by comparison to DLCA.

The process of reaction-limited colloid aggregation is characterized by several distinguishing features: the cluster structure, the aggregation kinetics, and the time evolution of the cluster-mass distribution. These features have been studied with analytical approaches, computer simulations, and by experiments.

The most widely used measure of the structure of RLCA clusters is the fractal dimension d_f. The fractal dimension determines the scaling of the mass of the cluster with its size.[9] We characterize the size of a cluster of mass M by its radius of gyration R_g and have $M=(R_g/a)^{d_f}$, where a is the radius of a single particle. We note that we assume that mass is measured in units of mass of a single particle, so that M represents the number of particles in the cluster. The fractal dimension d_f reflects properties of the radially averaged structure of the clusters.

Aggregates formed by RLCA from silica,[10] gold,[11] polystyrene latex,[12–15] and synthetic melanin[16] have all been studied experimentally. Their fractal dimensions have been measured using various methods, including static light scattering,[10–16] small-angle x-ray scattering,[17] and transmission electron microscopy[11] (TEM). Values of d_f varying between 2.05 and 2.20 have been found for these systems with a typical value being about 2.1. Computer simulations[18–20] modeling reaction-limited conditions also generate clusters with $d_f \approx 2.1$, in agreement with experiment.

In addition to the radially averaged properties of RLCA clusters as characterized by the fractal dimension, the anisotropy of the structure of aggregates has also been studied.[21] Using computer-simulated clusters, the anisotropy was also found to exhibit scaling properties, with a single characteristic length scale determined by the cluster size, and with exponents determined by d_f. Thus no additional parameters are needed to describe the scaling of the anisotropy of the structure of RLCA clusters.

Analytical approaches to the RLCA regime have focused on the Smoluchowski rate equation,[22,23] which describes the time evolution of the cluster mass distribution through a statistical characterization of the reaction kernel, or the aggregation rate of two clusters of different masses. Implicit in the use of the Smoluchowski equation is the assumption that the kernel is a function of the two cluster masses. The solution has been shown to exhibit dynamic scaling,[23,24] and can be written as

$$N(M)=M_n^{-2}\psi(M/M_n)\ , \tag{1}$$

where $N(M)$ is the number of clusters of mass M, and

$$M_n(t_a)=\frac{\sum_M N(M)M^n}{\sum_M N(M)M^{n-1}} \tag{2}$$

is the nth moment of the distribution and is a function of the time elapsed from the initiation of the aggregation process t_a. The time dependence of the cluster-mass distribution is contained in M_n only, while the scaling function $\psi(x)$ is time independent, reflecting the *shape* of the cluster-mass distribution. For a wide variety of kernels, the cluster-mass distribution has a power-law form with an exponential cutoff

$$N(M)=AM^{-\tau}\exp(-M/M_c)\ , \tag{3}$$

where the normalization is determined from the conservation of total mass $N_0=\sum_M N(M)M$, where N_0 is the number of primary colloidal particles. This gives

$$A=\frac{N_0 M_c^{\tau-2}}{\Gamma(2-\tau)}\ ,$$

where $\Gamma(\nu)$ is the gamma function. The value of τ depends on the form of the kernel. For RLCA, Ball *et al.*[8] used a geometric argument to determine the scaling of the kernel, and thus the value of τ. They predicted that $\tau=1.5$ with the cutoff mass growing exponentially, $M_c \sim e^{t_a/t_0}$, where t_0 is a sample-dependent time constant. Computer simulations of RLCA also predict a power-law distribution of the cluster mass, although there is disagreement about the value of τ. One study[18] suggested that $\tau \approx 1.5$, while another study[25] suggested that the exponent increases to a value closer to 2 for large t_a.

Experimentally, the shape of the cluster-mass distribution has been measured for several different colloid systems. Von Schultess, Benedek, and de Blois[12] studied the cluster-mass distribution of polystyrene colloids where the aggregation was induced by an antigen-antibody reaction, which results in reaction-limited aggregation. They found that $N(M)$ was well described by Eq. (3), with $\tau \approx 1.5$, although their data extended over a relatively limited range of mass, up to about $M \approx 10$. More recent studies of RLCA polystyrene latex induced by salt[26,27] also found a value of $\tau \approx 1.5$ with measurements extending to $M \approx 20$. The dynamic scaling of the cluster-mass distribution was also observed in these experiments. Dynamic light scattering studies[28,29] of colloidal silica aggregates produced by RLCA were interpreted by assuming a power-law shape for the cluster-mass distribution. The value of τ was reported to be $\tau \approx 2$. However, these results were based on an interpretation[30] of the dynamic light scattering data which ignored several salient features and thus must be viewed with extreme caution. Another study using TEM counting techniques[31] showed that the cluster-mass distribution for colloidal gold aggregated by RLCA has a power-law dependence, with $\tau \approx 1.5$. The measured distribution was also found to exhibit dynamic scaling, so that data measured at different times could be scaled onto a single curve. While the measurement extended over a wide range of cluster sizes, the statistical accuracy was limited, as is characteristic of

counting methods.

There have been several experimental measurements of the aggregation kinetics for RLCA. Dynamic light scattering was used to monitor the growth rate of colloidal gold,[11] and synthetic melanin,[16] and exponential growth was found for both. Care must be exercised in the interpretation of the dynamic light scattering data, because of the polydispersity in $N(M)$ and the contribution from rotations of clusters which lead to an additional dependence on the scattering wave vector. Nevertheless, the exponential kinetics persist, independent of these effects. The aggregation kinetics of colloidal silica have been studied using static light scattering[32] and were also found to be exponential for RLCA.

Reaction-limited aggregation has been explored for a variety of colloids. They all exhibit similar behavior, which is generally consistent with the theoretical predictions based on computer simulation or the solution to the Smoluchowski rate equations for RLCA. Nevertheless, some discrepancies remain, the most glaring of which is the value of the exponent for the cluster-mass distribution τ. Furthermore, a systematic study of the behavior of reaction-limited colloid aggregation for several different colloids, and a critical comparison of their properties, using both static and dynamic light scattering, has been lacking. In the following sections, we present a study of light scattering from colloidal aggregates, and show that static and dynamic light scattering are sensitive to several important characteristic features of the RLCA process. We use the results of this study to critically test the universality of the RLCA regime. In addition, we unambiguously determine the value of τ for all the experimental systems.

III. EXPERIMENTAL METHODS

We use both static and dynamic (or quasielastic) light scattering to study the colloidal aggregates. Static light scattering measures the time-averaged scattering intensity from the sample $I(q)$ as function of the scattering wave vector $q=(4\pi n/\lambda)\sin(\theta/2)$, where λ is the incident wavelength *in vacuo*, n is the index of refraction of water, and θ is the scattering angle. Dynamic scattering measures the temporal autocorrelation function of fluctuations in the scattering intensity resulting from the diffusive motion of the clusters.

We measure both the total scattered intensity and the autocorrelation function concurrently as functions of the scattering angle, and hence the scattering wave vector, using a photodetector mounted on the rotating arm of a goniometer. Data are typically collected at scattering angles between 10° and 150°, spaced approximately uniformly in the logarithm of q. The excitation source is the 488-nm line of an Ar^+ laser, so the accessible scattering vectors are $0.003 \le q \le 0.03$ nm^{-1}. For the colloidal gold samples, which strongly absorb the incident light, the intensity is maintained at less than 1 mW before entering the sample cell to avoid spurious heating effects.

The autocorrelation functions are measured with a 272-channel correlator. The decay time of the autocorrelation function varies both as q is changed and as the clusters grow. Thus, for most measurements, the sample time of the correlator is adjusted so that the measured autocorrelation function decays in magnitude by about one decade. We measure the intensity autocorrelation function $G_2(t)=\langle I(q,0)I(q,t)\rangle$, where t is the delay time and the angular brackets represent an ensemble average. We determine the normalized field autocorrelation function

$$g_1(t)=\langle E^*(q,0)E(q,t)\rangle/\langle |E(q,0)|^2\rangle ,$$

where $E(q,t)$ is the scattered field, through the use of the Siegert relationship,[33]

$$|g_1(t)|^2=F[G_2(t)/\langle I\rangle^2-1] , \tag{4}$$

where $\langle I\rangle$ is the average intensity and F is a constant determined primarily by the collection optics. The average intensity is measured by the correlator both directly and by baseline channels, which are delayed an additional 1024 delay times. The two measures typically agree to within 0.5%, and we routinely use the average intensity determined directly from the total detected signal. The autocorrelation functions are typically highly nonexponential. We determine their first cumulant, or the initial decay rate, given by the logarithmic derivative as $t\rightarrow 0$,[34]

$$\Gamma_1=-\left.\frac{\partial \ln g_1(t)}{\partial t}\right|_{t=0} . \tag{5}$$

Experimentally, we determine Γ_1 from a least-squares fit of the logarithm of $g_1(t)$ to a third-order polynomial.

We make the measurements *in situ* while the aggregation is in progress. Data are taken as a function of both the scattering vector q, and the aggregation time t_a. The slow aggregation rate of RLCA allows time for sufficient averaging to obtain a good measure of Γ_1 before the cluster size has changed substantially, even at the smaller values of q. However, if the autocorrelation functions are to be measured at very long delay times, or if data at many q but at the same t_a are to be obtained, the aggregation must be stopped to provide sufficient time to obtain the data without a change in the cluster sizes. This can only be done for colloidal gold. Its aggregation can be halted by the addition of a small amount of surfactant to the solution. We use the surfactant[35] sodium dodecyl-*o*-xylenesulfonate ($NaC_{12}OXYS$), at a final concentration of 10^{-3} M. It adsorbs on the surface of the gold particles, providing a steric stabilization that prevents the formation of any further bonds thus stopping the aggregation. The addition of the surfactant does not, however, change any of the scattering properties of the clusters, as confirmed by separate experiments.

We use three different types of colloids: gold, silica, and polystyrene. Each is a charge-stabilized aqueous system that can be aggregated under either diffusion-limited or reaction-limited conditions.

The colloidal gold is made by a reduction of a gold salt using sodium citrate, following a modified recipe due to Turkevich.[3,36] The primary particle radius is $a=7.5$ nm, and the initial volume fraction of the colloid as prepared

is $\phi_0=2.8\times10^{-6}$. The colloid is initially stabilized by surface adsorbed citrate ions. Aggregation is initiated by addition of pyridine, which is a neutral molecule that is adsorbed on the surface of the particles, displacing the citrate ions and reducing the stabilizing surface charge. The amount of pyridine added determines whether the aggregation is diffusion or reaction limited. For RLCA, the final concentration of pyridine was 9×10^{-6} M.

The colloidal silica used is Ludox-SM obtained from DuPont. It consists of particles with $a=3.5$ nm and, for these experiments, was diluted into two samples, one with $\phi_0=1.0\times10^{-3}$, the other $\phi_0=1.0\times10^{-5}$. The colloid is initially stabilized by SiO^- groups on the surface of the particles. The pH was adjusted to ≥ 11 by addition of NaOH to provide enough OH^- ions, which are needed to catalyze the formation of the particle bonds. Aggregation was initiated by addition of NaCl, which decreases the Debye-Hückel screening length, reducing the repulsive barrier between the particles. The final salt concentration was 0.6 M.

The polystyrene latex used was also commercially obtained, and had $a=19$ nm, and was diluted to $\phi_0=6.7\times10^{-6}$. This colloid is stabilized by charged carboxylic acid groups on the surface of the particles. Aggregation was initiated by adding NaCl to a concentration of 0.2 M, which decreases the Debye-Hückel screening length. The particle shape is deformed on bonding, presumably due to the large van der Waals attraction between the particles.[37]

The study of the regime of reaction-limited colloid aggregation requires considerable experimental care. The repulsive barrier between the colloid particles must be reduced only to the point that it is on the order of a few k_BT. If it is reduced too much the aggregation will be diffusion limited or will be in the intermediate regime and will rapidly revert to the diffusion limit; if it is not reduced enough, the aggregation will not proceed at all in a reasonable time. Thus a certain degree of experimental caution must be exercised to study RLCA: the glassware used must be carefully cleaned to avoid the ubiquitous problem of impurities which can adsorb on the colloid surface, changing the energy of repulsion. Our cleaning procedure entailed soaking the glassware in chromerge for about an hour, rinsing it with distilled water, and then with a dilute HCl solution, followed by a final rinse in distilled, deionized water. The amount of salt, acid, or pyridine added to initiate the aggregation must be adjusted slightly for each batch of colloid to obtain an aggregation that takes place in a reasonable amount of time. For the initial concentrations used here, this time is roughly 10 h. Faster rates lead to aggregation in the intermediate regime, while slower rates result in experiments lasting inordinately long times. Even with careful control of the cleanliness of our glassware and purity of our colloid solutions, we find in practice that the simplest way to achieve suitable RLCA conditions is to start with several samples of the colloid. Slightly different initial concentrations of the aggregating agent are added to each, and the size monitored during the initial stages. Some samples will aggregate too rapidly, crossing over to the diffusion-limited regime in a relatively short period of time, precluding the study of the RLCA regime over a sufficient length of time. Other samples may not aggregate at all during the course of the experiment. However, we always find suitable samples which exhibit RLCA kinetics over the entire experimental duration, and data are collected from these samples. This rather empirical method makes possible routine achievement of the true RLCA conditions over the duration of our experiments, which is typically about 10 h. The colloidal gold is particularly delicate, as the colloid degrades rapidly due to impurity absorption on the surface of the particles, making the results less reproducible. This problem was avoided by using a freshly prepared batch for each experiment.

There are several other experimental precautions that must be observed. The aggregation process is studied over several hours and a very wide distribution of cluster sizes is produced. Thus care must be taken to avoid differential sedimentation of the clusters during the measurement. To illustrate this problem, we can calculate the drift velocity of a cluster of mass M due to gravity. It is given by

$$v=\frac{2g}{9\eta}(\rho-\rho_0)a^2\left[\frac{R_h}{a}\right]^{d_f-1}, \tag{6}$$

where ρ is the density of the colloidal particles, ρ_0 is the density of water, g is the gravitational acceleration, and η is the water viscosity. Here R_h is the hydrodynamic radius of the cluster, which for our present purpose can be taken equal to R_g.

The cluster mass distribution for RLCA is highly polydisperse. Thus the larger clusters will sediment a much larger distance than the smallest clusters. For example, for gold, which has $\rho=19$ g/cm^3 and $a=7.5$ nm, a larger cluster, with a radius of $R_g\approx10$ μm, will have a gravitational drift velocity of ~21 mm/h. By contrast, a smaller cluster, with a radius of 0.1 μm, will have a drift velocity of only ~0.14 mm/h. This can substantially change the cluster-mass distribution at any height over the course of a few hours. Even for silica, which has a smaller density ($\rho\approx2.5$ g/cm^3 and $a\approx3.5$ nm), a moderately sized, 1-μm cluster has a drift velocity of ~0.4 mm/h, which is not negligible for an experiment that extends over a full day. To avoid the problem of differential sedimentation, our experiments are conducted in zero average gravity.[38] This was not achieved by doing them on the space shuttle. Rather, we used a long cuvette as a sample cell, filled it completely with the colloid, and sealed it at the top. The cell was then inverted every 15 min to achieve zero gravity on average, and thus eliminate any effects of sedimentation. This procedure is essential if the results are to be compared with the calculations of simulations, which ignore the consequences of gravitational sedimentation.

Finally, to compare the experimental measurements to the theoretical predictions, we must ensure that the process studied is truly one of aggregation rather than one of gelation. Due to their fractal nature, the aggregates occupy an increasing volume fraction of the solution as they grow, even though the total mass is conserved. If this

volume fraction approaches unity, gelation occurs. The physics of this gelation process is quite different from that of aggregation and cannot be compared to theoretical models for RLCA. Complete gelation occurs when the cluster volume fraction is roughly unity, and, if R_c is the radius of the largest cluster at the time of gelation, the required initial volume fraction is $\phi_0 \approx (a/R_c)^{3-d_f}$. For example, if $R_c \sim 10$ μm and $a=3.5$ nm, as for colloidal silica monomers, then $\phi_0 \approx 8\times 10^{-4}$ for gelation. Thus to follow the aggregation to later times, we must avoid gelation by ensuring that $\phi_0 \lesssim 10^{-5}$.

IV. LIGHT SCATTERING FROM RLCA AGGREGATES

To fully exploit the light scattering data obtained from colloidal aggregates and extract the maximum amount of useful information requires a careful analysis of both the static and dynamic light scattering data.[39] In this section, we develop a detailed, self-consistent description of both static and dynamic light scattering from RLCA aggregates. We compare calculations with experimental measurements of both the total intensity and the shape of the intensity autocorrelation function, obtained concurrently, at different scattering wave vectors. These experiments are performed on colloidal gold, since independent measurements have established many of the important features of its aggregation, including the fractal dimension of the clusters and the shape of the cluster-mass distribution. To obtain high quality data at several scattering angles from the same sample, the aggregation process is halted by the addition of surfactant. For our calculations, we make extensive use of clusters obtained from computer simulations using rules modeling reaction-limited colloid aggregation.

We obtain excellent agreement between our calculations and our data for both the static intensity and the shape of the autocorrelation function. The q dependence of the static intensity allows us to determine the structure factor of the clusters and their fractal dimension, as well as the radius of gyration of the average cluster in the distribution. Since dynamic light scattering is sensitive to the hydrodynamic radius R_h, we are able to independently determine the ratio $\beta=R_h/R_g$ from autocorrelation functions measured at small values of q. The shape of the autocorrelation functions measured at higher q is also sensitive to the contribution of rotational diffusion, allowing us to also determine the anisotropy of the structure of the clusters.

A. Static light scattering

The scattering intensity of a single cluster of mass M can be written as

$$I_M(q) \sim M^2 S(qR_g) F^2(q) . \tag{7}$$

We assume that the primary particles are sufficiently small that their form factor $F(q)=1$ for all experimentally accessible values of q. The scale invariance of the fractal clusters ensures that the structure factor $S(qR_g)$ is a function of the product qR_g only. The asymptotic behavior of the structure factor is

$$S(qR_g) \sim \begin{cases} 1, & qR_g \ll 1 \\ (qR_g)^{-d_f}, & qR_g \gg 1 . \end{cases} \tag{8}$$

Thus, for $qR_g \ll 1$, the clusters can be considered as point scatterers and the scattering is completely coherent, so that $I_M(q) \sim M^2$. By contrast, for $qR_g \gg 1$, the fractal correlations of the cluster structure are resolved, and $S(qR_g) \sim (qR_g)^{-d_f} \sim M^{-1} q^{-d_f}$ so that $I_M(q) \sim M q^{-d_f}$.

The shape of the structure factor is most sensitive to R_g in the crossover regime, when $qR_g \approx 1$. Here, the shape is determined by the finite extent of the fractal correlations imposed by the size of the cluster. We cannot experimentally measure the structure factor of a single cluster. Instead, we calculate $S(qR_g)$ from an average of several hundred computer-simulated RLCA clusters. For convenience, we parametrize the results by a polynomial form[39]

$$S(x) = (1 + C_1 x^2 + C_2 x^4 + C_3 x^6 + C_4 x^8)^{-d_f/8} , \tag{9}$$

where $x = qR_g$, $C_1 = 8/3d_f$, and $C_2 = 3.13$, $C_3 = -2.58$, and $C_4 = 0.95$ are obtained from a fit to the calculated structure factor. This expression has the correct asymptotic forms at both limits of x. Furthermore, the value chosen for C_1 ensures that $S(x \to 0) = 1 + x^2/3$, so that it follows the Guininer form as required at small x. The higher-order terms are required to correctly characterized the calculated shape of the structure factor, which exhibits a rather sharp crossover. While other, physically motivated, forms for the structure factor of fractal clusters have been proposed, the polynomial form in Eq. (9) has been shown to describe the scattering from computer-generated cluster more accurately.[40]

The experimentally measured scattering intensity is a weighted sum over the cluster-mass distribution

$$I(q) = \sum_M N(M) I_M(q) \sim \sum_M N(M) M^2 S(qR_g) . \tag{10}$$

For the cluster-mass distribution, we use the power-law form with an exponential cutoff, given by Eq. (3). We set the cluster-mass exponent to be $\tau = 1.5$, in accord with the results of TEM measurements of $N(M)$ for colloidal gold aggregates[31] produced by RLCA. We relate the cutoff mass M_c to an average cluster mass defined by the second moment of the cluster-mass distribution

$$M_2 = \frac{\sum_M N(M) M^2}{\sum_M N(M) M} . \tag{11}$$

For $\tau = 1.5$, we have $M_2 \approx 0.51 M_c$. We also define the average radius of gyration $\bar{R}_g = a M_2^{1/d_f}$, which is the only fitting parameter required to compare the calculated $I(q)$ with the experimental measurement. With this choice of $N(M)$, the scattered intensity also has the same asymptotic behavior as the structure factor for a single cluster. At small q, it is isotropic, independent of q, while at large q, it has a power-law shape $I(q) \sim q^{-d_f}$, reflecting the fractal dimension of the clusters.

The experimental data are only sensitive to the value of $\bar{R}_g$ when it exhibits a clear crossover from the power-law behavior at high q to the isotropic q-independent behavior at low q. To obtain experimental data in this regime, we add surfactant to stop the aggregation when the clusters are at a suitable size to experimentally access the crossover region. An example of the measured scattering intensity for clusters meeting these requirements is shown by the circles in Fig. 1. The crossover region extends over the entire range of accessible q, and only at very large q do the data appear to be linear on the logarithmic plot. The fit to Eq. (10) is shown by the solid line in Fig. 1, and is in excellent agreement with the data. The only fitting parameter is the average mass, and we find $M_2=1020\pm20$, which gives the average radius of gyration $\bar{R}_g\approx203$ nm. This value of M_2 or, equivalently, $\bar{R}_g$, which characterizes the cluster-mass distribution at time t_a, can now be used in fitting the dynamic light scattering data.

B. Quasielastic light scattering

Dynamic or quasielastic light scattering (QELS) measures the fluctuations of the scattered light, thereby probing the dynamics of the aggregates.[33,41] When $qR_g<1$, the fluctuations result from the translational diffusion of the clusters, while when $qR_g>1$, they result from both translational and rotational diffusion. To account for both of these contributions, the structure factor can be decomposed into spherical harmonics and the autocorrelation function can be calculated from these harmonics. The results obtained are in excellent accord with experimental measurements.[41] An alternate approach is to explicitly take advantage of the scaling properties of the clusters, and write the autocorrelation function as

$$g_1(t)=\frac{1}{I(q)}\sum_M N(M)M^2S(qR_g)\exp(-q^2D_{\text{eff}}t)\ . \qquad (12)$$

This is again a sum over the cluster-mass distribution, weighted by the scattering intensity of each cluster and by the decay of the autocorrelation function for each individual cluster. The decay rate for each cluster is determined by an effective diffusion coefficient $D_{\text{eff}}=Df(qR_g)$, where the translational diffusion coefficient is $D=\zeta/R_h$ with $\zeta=k_BT/6\pi\eta$. The contributions of rotational diffusion are included in $f(qR_g)$. When $qR_g\ll1$ rotational diffusion does not contribute, and $f(qR_g)\approx1$. When $qR_g\gg1$, rotational diffusion makes a substantial contribution, and $f(qR_g)\sim2$. We calculate $f(qR_g)$ using computer-simulated RLCA clusters. The structure factors are resolved into their spherical harmonics and the q-dependent effective-diffusion coefficient for each cluster is determined. We used 175 clusters of masses from 50 to 1460 particles, and obtained $f(qR_g)$ from the average.[39,41]

We note that in Eq. (12) we include the effects of rotations only in D_{eff} for each cluster. Thus we assume that the autocorrelation function from an individual cluster is strictly exponential in shape. This neglects the effects of rotational diffusion on the higher cumulants, and thus, Eq. (12) is exactly only to the first cumulant. However, this approximation is quite good. Since the aggregates formed by RLCA are so highly polydisperse, the nonexponential shape of the autocorrelation function is dominated by the effects of the cluster-mass distribution. This is confirmed by a calculation[42] of the second cumulant Γ_2 for the autocorrelation function of an individual cluster, which shows that $\Gamma_2/\Gamma_1^2\ll1$ for $qR_g\gg1$.

An example of an autocorrelation function obtained at low scattering vector is shown in Fig. 2. It was obtained at $\theta=15°$, corresponding to $q=0.00447\ \text{nm}^{-1}$, using the same sample whose static scattering was shown in Fig. 1. Using Eq. (3) for the cluster-mass distribution, and Eq. (9) for the structure factor, with $\bar{R}_g=203$ nm, as obtained from the static scattering, we calculate the autocorrela-

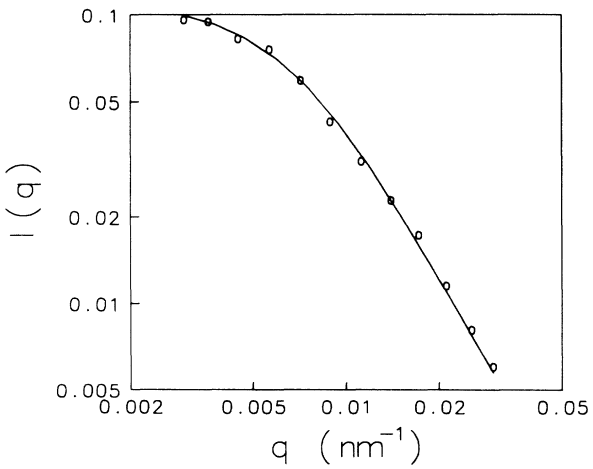

FIG. 1. Static light scattering intensity (in arbitrary units) from colloidal gold aggregates formed by RLCA. The data were taken when the sizes of the aggregates were not large enough for the intensity to exhibit a linear fractal scaling in the logarithmic plot. The solid curve is a calculation using Eqs. (3), (9), and (10) with $\bar{R}_g\approx203$ nm.

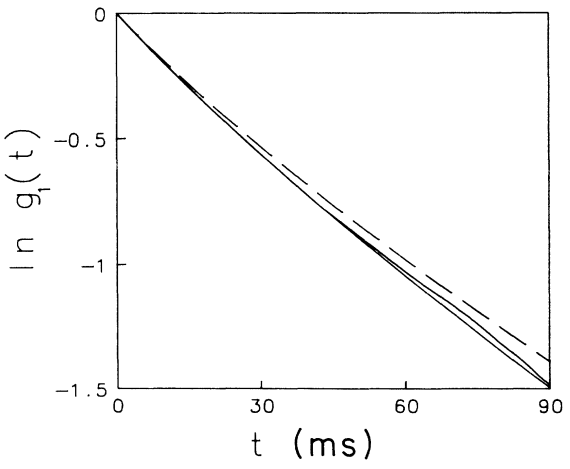

FIG. 2. Autocorrelation function measured at $\theta=15°$ for gold RLCA aggregates. The solid curve through the data is a fit using Eq. (12) and D_{eff}, which includes the effects of rotational diffusion. The fit and the data are hardly distinguishable. The dashed curve is the same calculation, but excluding the effects of rotational diffusion.

tion function using Eq. (12). The only unknown parameter is β, the ratio of the hydrodynamic radius of each cluster to its radius of gyration. This is used as a fitting parameter. We obtain $\beta=1.0$, which gives the excellent fit shown in Fig. 2. Since $q\bar{R}_g \approx 0.9$, $f(qR_g)\approx 1$, and rotational diffusion plays only a minor role as can be seen from the dashed curve shown in Fig. 2, which is a calculation using $D_{\text{eff}}=D$ for all the clusters. Thus the value obtained for β does not depend in any significant way on the contribution of rotational diffusion. The value obtained is in remarkably good agreement with the value of $\beta=0.97$ determined for computer-simulated RLCA clusters,[43] and is consistent with theoretical predictions.[44] It is also in agreement with that obtained for colloidal silica using light scattering, after the effects of polydispersity are properly included.[44–46]

At larger q, $f(qR_g)>1$, and the effects of rotational diffusion significantly modify the decay of the autocorrelation function. However, we are able to account for these effects by using the calculated form for $f(qR_g)$. As an example, we show in Fig. 3 the autocorrelation function measured at $\theta=96°$, which corresponds to $q=0.0255$ nm^{-1}. We obtain excellent agreement with the data when we calculate the shape of the autocorrelation function using Eq. (12), with $\beta=1.0$ and $\bar{R}_g=203$ nm. Since $q\bar{R}_g \approx 5.3$, rotational effects are clearly important, as can be seen by the dashed curve in Fig. 3, which is the calculation without rotations, and deviates considerably from the data. Indeed, by including the effects of rotational diffusion in calculating the autocorrelation function, we can obtain excellent agreement between our calculations and the data at all values of q. We illustrate this in Fig. 4, where we show the values of $\bar{R}_g$ obtained from using Eq. (12) to fit the autocorrelation functions at 11 angles from 15° to 161°. In performing the fits, we have set $\beta=1.0$ and have included the effects of rotational diffusion in $f(qR_g)$. Thus the only fitting parameter is

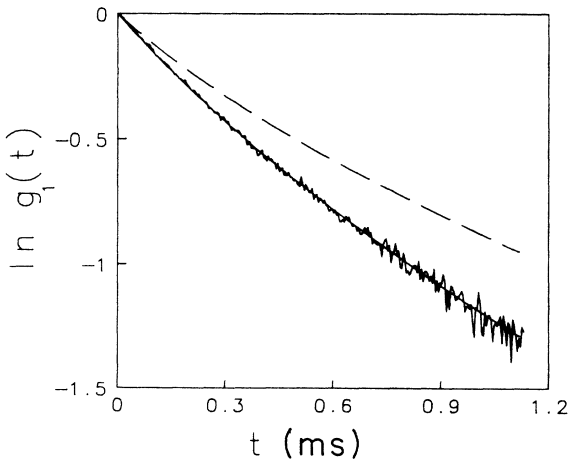

FIG. 3. Autocorrelation function measured at $\theta=96°$ for gold RLCA aggregates. The solid curve through the data is a fit using Eq. (12) and D_{eff}, which includes the effects of rotational diffusion. The dashed curve is the same calculation, but excluding the effects of rotational diffusion, which are significant in this case.

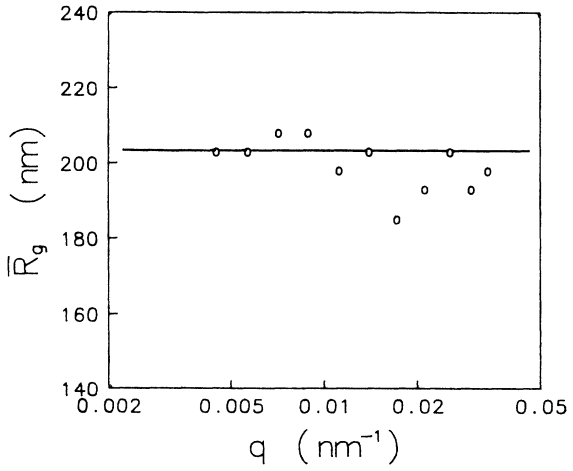

FIG. 4. Values obtained for $\bar{R}_g$ from fitting the autocorrelation function at different scattering wave vectors. The solid line shows the value of $\bar{R}_g=203$ nm, obtained from fit to the static scattering intensity shown in Fig. 1.

$\bar{R}_g$. Since the same sample is used for all these measurements, the same value of $\bar{R}_g$ should be obtained. The deviation found in the fitted $\bar{R}_g$ is less than 6%, demonstrating the excellent agreement.

In this section, we have developed a self-consistent interpretation of the static *and* dynamic light scattering data from RLCA aggregates. The same value of the average radius of gyration $\bar{R}_g$ is obtained from the fits to the data for both types of light scattering. In addition, we are able to determine the value of $\beta=R_h/R_g$ for RLCA clusters. However, we emphasize that we have assumed that the form of the cluster-mass distribution is given by a power law with an exponential cutoff, as in Eq. (3). Furthermore, we have taken $\tau=1.5$, based on independent TEM measurements for colloidal gold. While this assumption gives excellent agreement with the data, the results are not particularly sensitive to the value of τ used. Indeed, nearly as good fits are obtained with values of τ between 1.4 and 1.7, albeit with slightly different values of $\bar{R}_g$. In the following sections we develop an additional form of analysis, which exploits more experimental data, and allows us to unambiguously confirm the chosen value of $\tau=1.5$.

V. SCALING OF THE FIRST CUMULANT

As shown in the previous section, we can self-consistently describe both the static and dynamic light scattering from the same sample. These measurements, however, were made at a single time t_a, and thus do not provide any information about the kinetics. Furthermore, the value of the cluster-mass exponent τ could not be unambiguously determined from either measurement. In this section, we present an alternate analysis of dynamic light scattering data that provides information about both the kinetics of the aggregation process as well as the cluster-mass exponent. We consider the first cumulant of the autocorrelation function, and show that data ob-

tained at all aggregation times t_a and at all values of q can be scaled onto a single master curve. This is accomplished by exploiting the dynamic scaling of the cluster-mass distribution. The shape of this master curve depends critically on key features of the aggregation process, including the structure and anisotropy of the aggregates and the shape of their cluster-mass distribution. Thus the master curve can also be used to critically compare the aggregation behavior of completely different colloids, as we show in Sec. VI.

Rather than using the first cumulant of the autocorrelation function directly, it is convenient to remove the trivial q^2 dependence by determining the average effective-diffusion coefficient $\bar{D}_{\rm eff}=\Gamma_1/q^2$. Using Eqs. (5) and (12),

$$\bar{D}_{\rm eff}=\frac{\sum_M N(M)M^2S(qR_g)D_{\rm eff}}{\sum_M N(M)M^2S(qR_g)} . \tag{13}$$

This is simply an average of the effective-diffusion coefficients of the individual clusters, which include the effects of rotations, weighted by the cluster-mass distribution function and the static scattering intensity. Both the structure factor and $D_{\rm eff}$ are functions of q, so that $\bar{D}_{\rm eff}$ also is a function of q. It is this q dependence which provides the sensitivity to the features of the aggregation process.

To determine this q dependence, and the origin of the sensitive dependence on the cluster-mass distribution and the properties of the clusters, it is instructive to first evaluate Eq. (13) analytically. This can be accomplished by making several simplifying assumptions. We neglect the contribution of rotational diffusion, thus set $D_{\rm eff}=D=\zeta/\beta R_g$. We assume $N(M)=A'M^{-\tau}$ up to a cutoff mass M_c, and take $N(M)=0$ for $M>M_c$, where $A'=(2-\tau)N_0/M_c^{2-\tau}$. Finally, we set $S(qR_g)$ equal to its asymptotic forms, given by Eq. (8). Replacing the summations in Eq. (13) by integrals, we have,

$$\bar{D}_{\rm eff}=\frac{\zeta}{a}\frac{\int_1^u M^{2-\tau-1/d_f}dM+u\int_u^{M_c}M^{1-\tau-1/d_f}dM}{\int_1^u M^{2-\tau}dM+u\int_u^{M_c}M^{1-\tau}dM} , \tag{14}$$

where $u=(aq)^{-d_f}$ is the mass of the cluster with $R_g=q^{-1}$. Physically, this represents the boundary of the two different regimes of the structure factor in Eq. (8). Thus $\bar{D}_{\rm eff}$ is independent of q in two limits: the first case is when $q<R_c^{-1}$, where $R_c=aM_c^{1/d_f}$ is the radius of gyration of the largest cluster. Then only the first integrals in both the numerator and denominator of Eq. (14) contribute, with the upper limit in each case being M_c, which is independent of q. The other two integrals are both identically zero. Here, all the clusters are small enough that their internal fractal structure is never probed, and their scattering intensity is then proportional the square of their masses. The second case is when $q>a^{-1}$, and the internal structure of all the clusters is resolved. (We assume that even the clusters of mass $M=1$ scatter as fractals.) Here, only the second of the two integrals in both the numerator and denominator contribute, with the lower limit in each case being 1, again independent of q. The first integrals are both identically zero.

More generally, the value of q lies in between these two limits and all four integrals contribute, resulting in a q dependence for $\bar{D}_{\rm eff}$. The value of τ determines the actual shape of this q dependence. Note, however, that if $d_f=2.1$ and $\tau=1.5$, the exponent of the second integrand in the numerator is very close to -1, leading to a very weak dependence of the result on either of the limits of the integration. Physically, this reflects the fact that although the larger clusters scatter more strongly, this is almost exactly compensated by the larger number of the smaller clusters resulting from the power-law cluster-mass distribution. Thus clusters of all mass contribute nearly equally to the integral. Furthermore, this sensitivity ensures that the contribution of rotational diffusion will be significant and cannot be ignored. As τ increases above 1.5, this integral is increasingly dominated by its lower limit, the clusters of mass u. The contribution of rotational diffusion is important for these clusters, and thus cannot be ignored. As τ approaches 2, the exponent of the second integrand in the denominator approaches -1, and it becomes increasingly sensitive to both of its limits. Thus for all values of τ relevant to RLCA, $\bar{D}_{\rm eff}$ is very sensitive to all the clusters in the distribution.

Performing the integrals in Eq. (14) exactly, we obtain, after some manipulation,

$$\bar{D}_{\rm eff}=\frac{\zeta}{a}\frac{(u^{3-\tau-1/d_f})/(3-\tau-1/d_f)+u^{3-\tau-1/d_f}[(M_c/u)^{2-\tau-1/d_f}-1]/(2-\tau-1/d_f)}{(u^{3-\tau}-1)/(3-\tau)+u^{3-\tau}[(M_c/u)^{2-\tau}-1]/(2-\tau)} . \tag{15}$$

In the limit of $M_c/u\to\infty$, the M_c/u term in the numerator can be neglected if $\tau>2-1/d_f$. Furthermore, if $\tau<2$ and $u\gg1$, a simple power-law q dependence results, $\bar{D}_{\rm eff}\propto q^{\alpha}$, with $\alpha=1-(2-\tau)d_f$, as has been suggested previously.[30] However, this simple q dependence is strictly true *only* in the limit of $M_c/u\to\infty$. In practice, it requires unrealistically large values of M_c to be valid whenever τ is near either $2-1/d_f$ or 2. Thus $\bar{D}_{\rm eff}$ never exhibits a simple power-law dependence on q and any attempt to use this type of behavior to extract a value of τ is bound to fail. Furthermore, the contribution of rotational diffusion cannot be neglected in determining the q dependence of $\bar{D}_{\rm eff}$.

To determine the true shape of $\bar{D}_{\rm eff}(q)$, we numerically evaluate the expression in Eq. (13). We use a power-law cluster-mass distribution with an exponential cutoff, as

given in Eq. (3). Since all clusters can make a significant contribution with a power-law distribution, we use Eq. (9) for the structure factor and include the higher-order terms to properly account for clusters with $qR_g \approx 1$. Similarly, we include the effects of rotational diffusion through the use of the scaling form for $D_{\rm eff}(qR_g)$, calculated from computer-simulated RLCA clusters. In Fig. 5, we show the results of these calculations for $\tau = 1.5$ and $a = 7.5$ nm, which is suitable for the colloidal gold. The calculations are shown for several different values of the cutoff mass: (a) $M_c = 10^4$, (b) $M_c = 10^5$, and (c) $M_c = 10^6$. For each curve, the asymptotic regions, where $\bar{D}_{\rm eff}$ is independent of q, can clearly be seen. The beginning of the asymptotic region at high q, determined by the value of a, remains at the same value of q. By contrast, the beginning of the asymptotic region at low q, which reflects the value of M_c, occurs at increasing lower values of q as the average cluster size grows. In fact, $R_c = aM_c^{1/d_f}$ sets a natural length scale for $\bar{D}_{\rm eff}$, as it must because of the dynamic scaling of the cluster-mass distribution. We can exploit this fact to scale all the curves onto a single master curve. For convenience, we choose $\bar{D} = \bar{D}_{\rm eff}(q=0)$ as the scaling parameter, which sets the characteristic length scale as $\bar{R}_h = \zeta/\bar{D}$, which scales with R_c, and is the average hydrodynamic radius that would be determined from the first cumulant of a QELS measurement as $q \to 0$. Thus, in Fig. 5(d), we plot $\bar{D}_{\rm eff}/\bar{D}$ as a function of $q\bar{R}_h$ for each of the three curves for the different M_c. A single master curve is obtained, except at high values of $q\bar{R}_h$, where the individual curves deviate, reflecting their different upper cutoffs due to the different values of R_c/a for each case. When $R_c/a \to \infty$, the asymptotic limit of the master curve is reached, and each of the individual curves falls on this curve up to the point where $q\bar{R}_h \sim \bar{R}_h/a$. Indeed, it can be shown that, if $N(M)$ has a scaling form Eq. (1), $\bar{D}_{\rm eff}/\bar{D}$ is a function of $q\bar{R}_h$ only.[47]

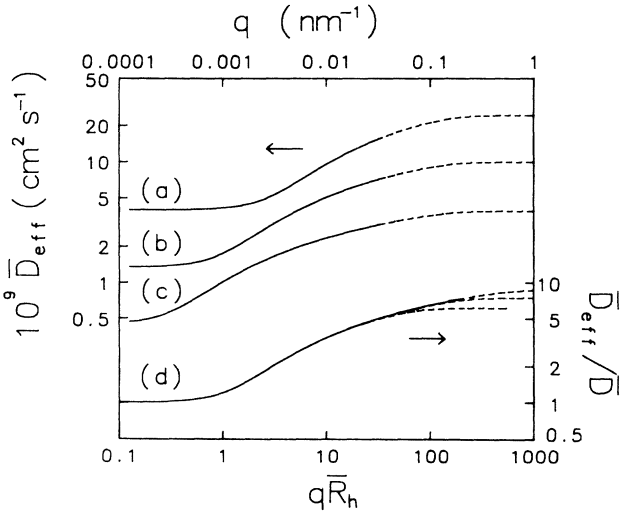

FIG. 5. Calculated $\bar{D}_{\rm eff} = \Gamma_1/q^2$ as a function of q using Eq. (13), with (a) $M_c = 10^4$, (b) $M_c = 10^5$, and (c) $M_c = 10^6$. The scale for $\bar{D}_{\rm eff}$ is on the left and the scale for q is on the top. The experimentally accessible range of q extends to about 0.03 nm^{-1}, after which the calculated curves are represented by dots. The three curves are scaled onto a master curve (d) as $\bar{D}_{\rm eff}/\bar{D}$ vs $q\bar{R}_h$, whose scales are on the bottom and the right of the plot.

The scaling of the separate curves has an important consequence for experimental measurements. The experimentally accessible range of q is limited, extending over $0.003 \le q \le 0.03$ nm^{-1}. However, repeating the measurements at later times, when M_c has increased, allows us to explore different portions of the full shape of the asymptotic master curve. Then by scaling these different data sets together, a single master curve can be obtained. Since, even for the largest q achieved experimentally, $qa \ll 1$ for all the colloids used, all the experimental measurements fall on the asymptotic curve.

The utility and importance of the master curves come from their sensitivity to the details of the aggregation process. These details include the shape of the cluster-mass distribution, the structure factor of the clusters, and the anisotropy of their structure as reflected by the contribution of rotational diffusion. To illustrate this sensitivity, we show, by the solid lines in Fig. 6, the calculated master curves for several different values of the cluster-mass exponent τ. In addition, we also show by the dashed lines the master curves that would be obtained with the same values of τ if the effects of rotational diffusion were not included, by setting $D_{\rm eff} = D$. For $q\bar{R}_h < 1$, the curves are indistinguishable. However, as $q\bar{R}_h$ becomes appreciably larger than 1, the shapes of the master curves depend markedly on the value of τ. In addition, the inclusion of rotational diffusion is also clearly reflected in their shapes. These examples illustrate the sensitivity of the master curves to both the structure of the clusters and the shape of the cluster-mass distribution, and demonstrate how the master curves can be used to probe the features of the RLCA process.

To illustrate how the experimental master curve is obtained, we again use colloidal gold. To extend the limited range of q that can be accessed experimentally, we must

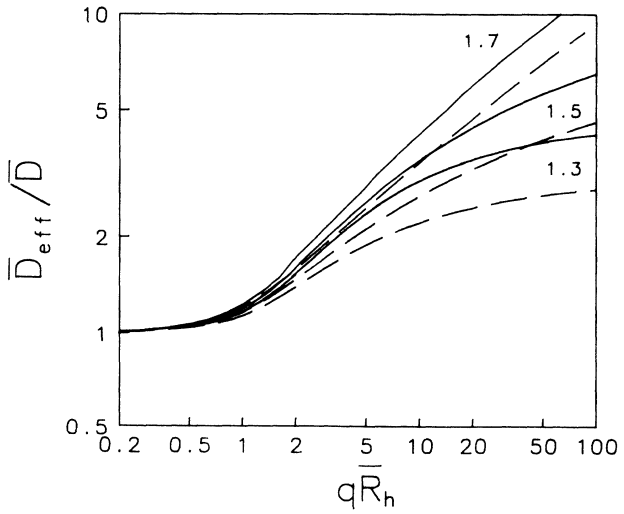

FIG. 6. Calculated $\bar{D}_{\rm eff}/\bar{D}$ for several different values of τ, each with (solid curves) and without (dashed curves) the effects of rotational diffusion.

determine $\bar{D}_{\rm eff}(q)$ at many times during the aggregation, corresponding to different values of M_c. This is accomplished by initiating the aggregation, and repeatedly measuring the first cumulant at a series of different angles as the aggregation proceeds. Because the aggregation rate is so slow, it is possible to collect sufficiently good data at each angle before the size of the average cluster has changed significantly. However, it is not possible to collect data at all angles, to obtain a complete set of $\bar{D}_{\rm eff}(q)$, before M_c has changed. Instead we interpolate between the measurements of the first cumulants at each angle, to obtain sets of data, each giving $\bar{D}_{\rm eff}(q)$ measured at the same time t_a and thus reflecting the same value of M_c. This corresponds to a single calculated curve in Fig. 5. We find experimentally that $\bar{D}_{\rm eff}$ increases exponentially in time at each q, and use this behavior for the interpolation. Seven sets of data obtained in this fashion are shown in Fig. 7 with each t_a labeled.

To experimentally determine the value of $\bar{D}$ for each data set would require a measurement at inaccessibly low values of q. Instead, data are scaled empirically using a single parameter for each data set. This corresponds to $\bar{D}=\zeta/\bar{R}_h$, and reflects the length scale of the largest cluster of the distribution at time t_a of the data set. On the logarithmic plot in Fig. 7, this scaling corresponds to shifting each data set along its diagonal. We can always obtain sufficient data that there is considerable overlap between successive data sets, so that the determination of the scaling parameters is unambiguous.

In Fig. 8, we plot the resultant master curve obtained in this fashion from the data shown in Fig. 7. All the data sets do indeed lie on a single master curve, as expected. We also plot the calculated master curves, shown previously in Fig. 6, for the three different values of τ, including the effects of rotational diffusion. We emphasize that there is no free parameter in comparing the data to the calculation. Excellent agreement is obtained between the experimental data and the calculated master curve, allowing us to determine that $\tau=1.5\pm0.05$. These results confirm the value of τ obtained previously using TEM

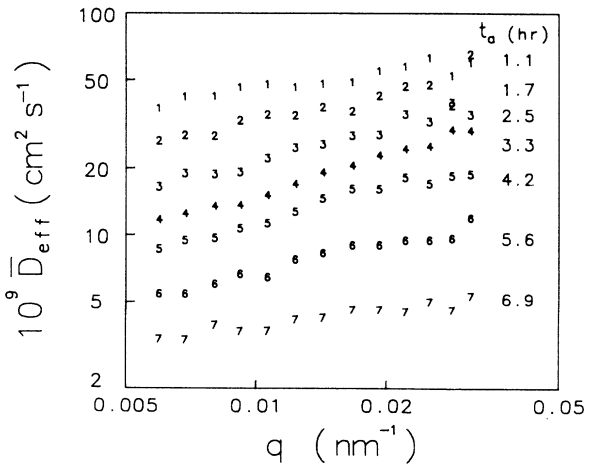

FIG. 7. Measured data for $\bar{D}_{\rm eff}$ as a function of q, taken at different times t_a, for colloidal gold prepared under RLCA conditions.

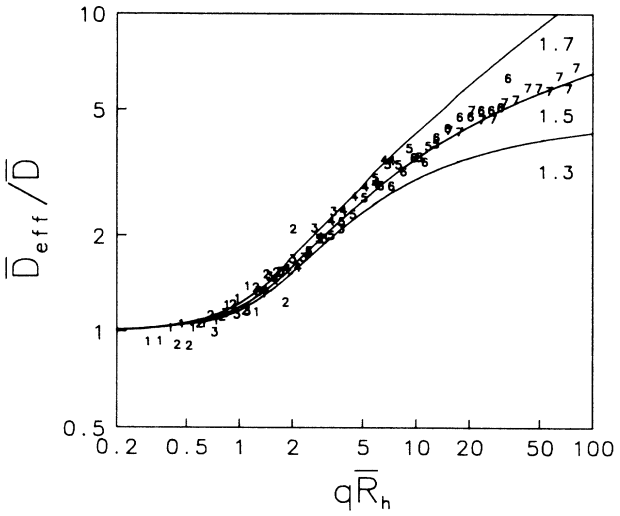

FIG. 8. Data from Fig. 7 scaled onto a master curve, by multiplying each of them by a factor of $\bar{R}_h/\zeta$, and plotted as a function of $q\bar{R}_h$. An $\bar{R}_h(t_a)$ is obtained for each data set such that it overlaps with the others. The solid lines are the same calculated master curves as shown in Fig. 6, with rotational effects included.

counting techniques.[31] However, these light scattering results have substantially better statistical accuracy. Furthermore, the value of τ is in excellent agreement with the theoretical prediction based on the Smoluchowski equations.[8] Finally, we again emphasize that the effects of rotational diffusion must be included to correctly compare the experimental data with the calculations.

We can also determine the kinetics of the aggregation directly from the scaling used to obtain the master curve. The scaling parameter $\bar{R}_h$ corresponds to the average hydrodynamic radius that would be measured in the limit $q\rightarrow0$, and thus reflects an accurate measure of the average cluster size of the distribution at t_a. In Fig. 9, we

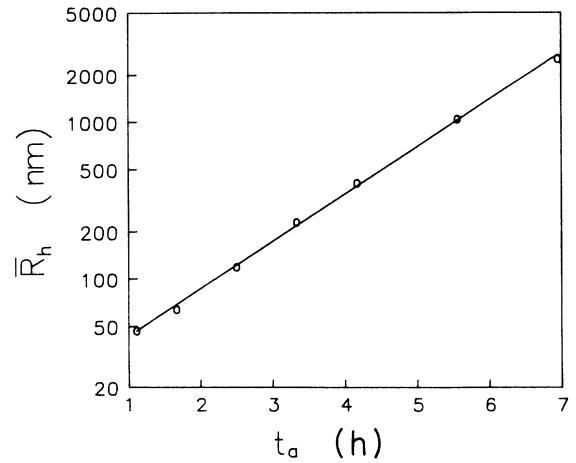

FIG. 9. Scaling factor $\bar{R}_h$ as a function of aggregation time t_a obtained from the scaling shown in Fig. 8 that would be measured at $q=0$. $\bar{R}_h$ represents the average hydrodynamic radius. The solid line is a fit giving an exponential form for the aggregation kinetics.

plot $\bar{R}_h$ as a function of t_a on a semilogarithmic scale. The linear behavior indicates that $\bar{R}_h \sim e^{t_a/t_0}$, so that the average hydrodynamic radius grows exponentially. This is also in agreement with the prediction from the solution of the Smoluchowski equations.

VI. UNIVERSALITY OF REACTION-LIMITED COLLOID AGGREGATION

The light scattering data discussed above provides a measure of the features of the aggregation process, independent of the material details of the colloid, thereby allowing RLCA of different colloids to be compared.[5,6] The static light scattering from different colloids provides a means to compare the fractal dimension of the clusters, while the time dependence of the scaling factors used to construct the master curves provides a means to compare the kinetics of the aggregation process. Finally, the master curves themselves provide a means of comparing several features of the RLCA process, including the cluster-mass distributions, the structure factor of the aggregates, and their anisotropy. All material specific parameters, such as the primary particle size, have been scaled out of the master curve, providing a critical comparison, with no free parameters.

To investigate this universality, we use three very different colloids: gold, silica, and polystyrene latex. Each is comprised of a different material, each is stabilized by different functional groups, each is aggregated by different methods, and each forms completely different interparticle bonds upon aggregation. However, the aggregation of each colloid can be controlled to obtain either $E_b \ll k_B T$ or $E_b \gtrsim k_B T$, allowing both diffusion-limited and reaction-limited colloid aggregation to be achieved.

Light scattering data from the silica and polystyrene colloids were collected in the same fashion as for the gold colloids discussed in Sec. V. Autocorrelation functions of the intensity fluctuations were measured repeatedly at different angles as the aggregation proceeded. The static light scattering intensity was measured concurrently, allowing the fractal dimension to be determined independently. Caution was exercised to avoid differential sedimentation effects by inverting the sample cells every 15 min. Since the scattering intensity from the silica is so weak, two samples were used. The first sample had a larger initial volume fraction of $\phi_0 = 1.0 \times 10^{-3}$, and its aggregation was followed until $\bar{R}_h \lesssim 1$ μm. The volume fraction of the clusters is still $\ll 1$, so that gelation is not approached. The high concentration of colloidal particles increases the scattering intensity of the clusters when their size is small compared with q^{-1}, enabling reliable data to be obtained at early times of the aggregation, when $q\bar{R}_h < 1$. The second sample had a lower initial volume fraction $\phi_0 = 1.0 \times 10^{-5}$. Data from this sample were collected only after $q\bar{R}_h \geq 1$, when the scattering intensity was sufficiently large. Here, the lower value of ϕ_0 ensured a sufficiently small volume fraction of clusters so that the aggregation could be studied to $\bar{R}_h \approx 5$ μm without approaching gelation. We emphasize, however, that the scaling method used here is still applicable using the two separate samples since the *shape* of the cluster-mass distribution exhibits a scaling form, and is unchanged for the two samples.

Master curves were produced from the dynamic light scattering data from the silica and polystyrene following the procedure described in Sec. V for the gold, and all three curves are plotted in Fig. 10. As can be seen, the master curves from the three different colloids are completely indistinguishable. We emphasize again that these master curves were determined independently for each colloid, and that the normalization removes all features specific to the individual colloids from the master curves so that there are no adjustable parameters in their comparison. The similarity of the master curves is striking evidence in support of the universality of reaction-limited colloid aggregation. This conclusion is independent of any theoretical interpretation or calculation of the shape of the curves.

The solid line in Fig. 10 is the calculated shape of the master curve assuming that $\tau = 1.5$, and is in excellent agreement with the experimental data. This confirms our ability to describe the process of RLCA and the structure of the resultant aggregates. Furthermore, it demonstrates convincingly and unambiguously that $\tau = 1.5$ for RLCA.

The static scattering from the three colloids also illustrates the universality of RLCA, as shown in Fig. 11. The data were all obtained when $q\bar{R}_h > 1$, so that the fractal structure of the clusters is clearly resolved, as indicated by the straight lines in the logarithmic plot. From the slopes the fractal dimensions are determined: $d_f = 2.10$ for gold, $d_f = 2.12$ for silica, and $d_f = 2.13$ for polystyrene. To within experimental error, the fractal dimensions are identical, yielding $d_f = 2.10 \pm 0.05$ for RLCA aggregates, where the error limits reflect our estimate of the total experimental variations.

The aggregation kinetics for each colloid were deter-

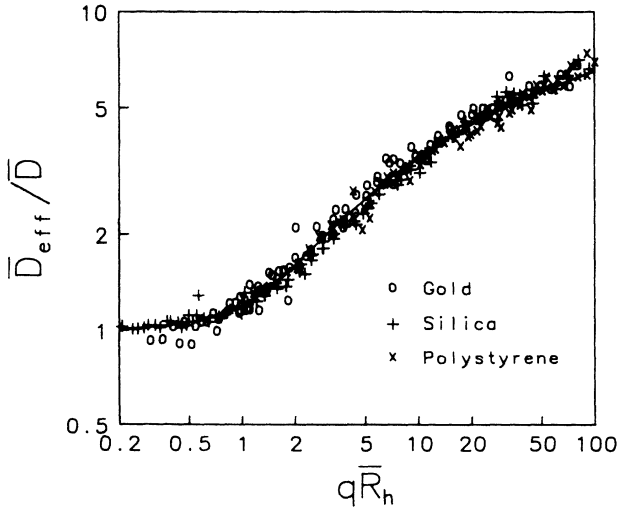

FIG. 10. Master curves obtained independently for gold (○), silica (+), and polystyrene (×) for RLCA. The solid curve is the calculation with $\tau = 1.5$.

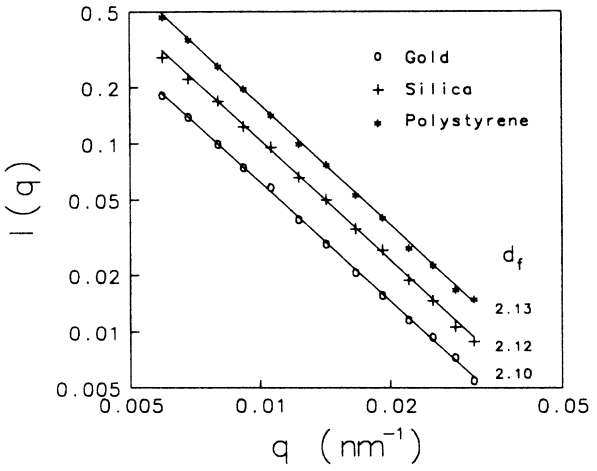

FIG. 11. Static light scattering from RLCA aggregates of gold (○), silica (+), and polystyrene (*). The measured fractal dimensions are gold, $d_f=2.10$; silica, $d_f=2.12$; and polystyrene, $d_f=2.13$.

mined from the time dependence of the scaling factor used to obtain the master curves. We plot $\bar{R}_h$ as a function of aggregation time t_a in Fig. 12. The kinetics for both the gold and silica have identical forms, with exponential growth $\bar{R}_h \sim e^{t_a/t_0}$ as indicated by the linear behavior in the semilogarithmic plot. The colloidal silica data were taken with the first sample, and stop at $\bar{R}_h \lesssim 1000$ nm. The different slopes reflect the different aggregation time constants t_0 for each colloid, which are determined by the single particle sticking probability P and by the initial particle concentration N_0.

The kinetics of the polystyrene colloids are also exponential, but appear to have two distinct time constants, with t_0 decreasing by a factor of about 3 after approximately 1 h. The polystyrene colloids are unique among the colloids used in this work in that they deform on aggregation.[37] This increases the radius of curvature of the particles, which in turn increases the interaction energy between two approaching particles, decreasing the reaction rate. Nevertheless, the form of the aggregation kinetics for the polystyrene is still best described as exponential, in agreement with that of the other colloid systems.

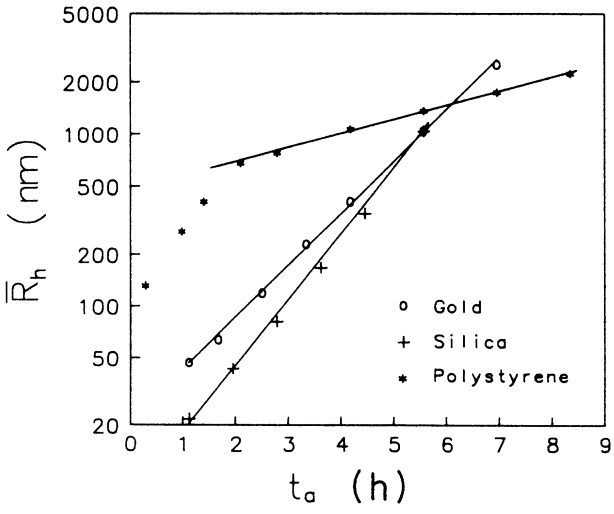

FIG. 12. Kinetics of RLCA aggregation of gold (○), silica (+), and polystyrene (*). The scale of $\bar{R}_h$ is logarithmic to show the exponential growth.

The behavior of the light scattering data from each of these three completely different colloids is identical. The similarity of the static light scattering from each colloid shows that the clusters formed in each case have the same fractal dimension. The similarity in the form of the kinetics for each colloid shows that they all exhibit exponential growth of the average cluster size. Perhaps most convincingly, the existence of the master scaling curves of identical shape for each colloid shows that the properties of the aggregates are identical: their cluster-mass distribution is the same, their structure factor is the same, and the anisotropy of the aggregates is the same. Thus we conclude that reaction-limited colloid aggregation is a universal process, independent of the chemical details specific to individual colloid systems.

VII. COMPARISON TO OTHER RESULTS

The process of reaction-limited colloid aggregation is characterized by several distinguishing features. It occurs when the sticking probability between two particles is very low, and thus its rate is much slower than would be the case if the repulsive barrier were eliminated entirely. The clusters formed are fractal and have $d_f=2.10\pm0.05$. The growth of the average cluster size is exponential in time. The shape of the cluster-mass distribution can be described by a power law, with an exponential cutoff. The cluster-mass exponent is $\tau=1.5\pm0.05$. This paper presents strong evidence that these features of RLCA are universal, and should therefore apply to other colloids aggregated under reaction-limited conditions. There have, however, been several reports of RLCA which appear to produce results at odds with those reported in this paper. It is therefore important to attempt to resolve any inconsistencies to determine the extent of the universality of RLCA.

One feature of RLCA that has been the subject of some debate is the value of the cluster-mass exponent τ. Several different values have been reported from computer simulations. Brown and Ball[18] performed an early simulation and found $\tau\approx1.5$. Meakin and Family[25] reported that τ was closer to 1.8, but further analysis of their data, which includes the exponential cutoff in $N(M)$, suggests that τ was closer to 1.5 at early times, but then rose to a value closer to 1.7 at later times. The origin of the discrepancy between the two different simulations is unclear.

There have also been other values of τ reported for colloidal silica, based on the analysis of dynamic light scattering data. Martin and Schaefer[28,29] compiled a scaling plot similar to those reported here, and obtained $\tau\approx2.0$. However, their data are significantly different

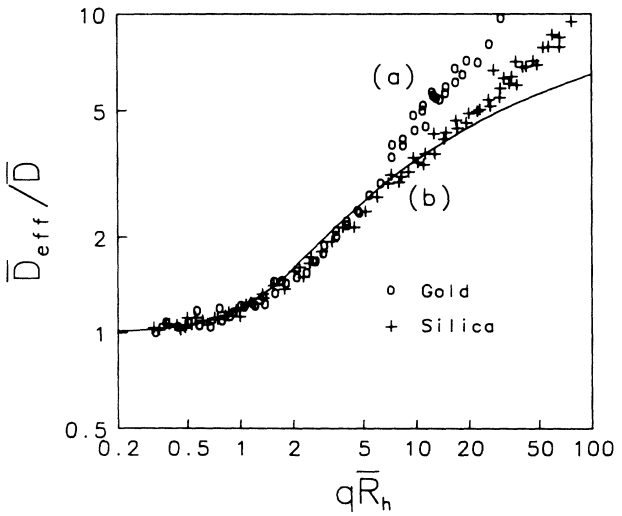

FIG. 13. Master curves obtained for (a) gold and (b) silica RLCA aggregates with sedimentation effects due to gravity. The initial volume fraction for the silica is $\phi_0 \approx 10^{-3}$. The differential settling rates of the clusters change the cluster-mass distribution, leading to the change in shape of the master curve. The calculated shape without gravitational settling is shown, for comparison, by the solid curve.

from the silica data presented in this paper. A key feature of our master curves is the apparent saturation of the data at large $q\bar{R}_h$. The data rise fairly rapidly when $q\bar{R}_h > 1$, but then begin to saturate and rise much more slowly as $q\bar{R}_h$ approaches 100. In fact, this behavior is observed for the master curves calculated for all τ between 1.5 and 2.0 By contrast, the data reported by Martin and Schaefer[28,29] continue to rise with $q\bar{R}_h$, never exhibiting any saturation.

There are two possible origins of this discrepancy. The first possibility is the problem of differential sedimentation. This will modify the cluster-mass distribution, and will presumably affect the aggregation process. It certainly modifies the shape of the master curve obtained. In Fig. 13(a), we show the master curve obtained for gold using the same procedure as before. Here, however, the sample was *not* inverted every 15 min to avoid the effects of gravity and attain $g=0$ on average. As can be seen in Fig. 13(a), the shape of the master curve obtained is markedly different. Instead of saturating at large $q\bar{R}_h$, as the gravity-free curves do, the data continue to rise, with a slope of about 0.45. Even though the density mismatch with the silica is much less than with the gold, a similar effect is obtained with a silica sample if differential sedimentation is not eliminated, as shown in Fig. 13(b). These results were obtained under similar conditions as those reported by Martin,[29] using $\phi_0 \approx 10^{-3}$, and the shape of the master curve in Fig. 13(b) is similar to that reported by him. The data again continue to rise with constant slope and no observable saturation. However, the slope is less than that of gold data obtained under gravity. The effects of differential sedimentation are always present unless the experiment is carried out in space under microgravity conditions or gravity is removed by the methods used here. However, these effects are not included in the simple models developed to account for RLCA. Thus the value of τ obtained from the experimental master curves without elimination of the effects of the differential sedimentation cannot be reliable.

A second possible problem may arise from the relatively large initial concentrations used in Martin and Schaefer's experiments. These authors present the same data in two separate publications,[28,29] but the initial concentration is reported as $\phi_0 \approx 10^{-2}$ in one[28] and $\phi_0 \approx 10^{-3}$ in the other,[29] making the true initial concentration impossible to determine. Nevertheless, at any of these high concentrations, gelation will occur for rather small $\bar{R}_h$. Indeed, they report that their sample does gel,[29] and in our experiments we observe very large clusters, of sizes on the order of several millimeters, at later times. Gelation is clearly a different process than aggregation, and will, in fact, produce cluster-mass distribution[23] with $\tau > 2$. Thus it is also possible that both the previous reported results,[28,29] and the results in Fig. 13(b) represent a crossover from aggregation to gelation, which will again modify the shape of the master curve. As a result we must conclude that $\tau = 1.5$ for true reaction-limited colloid aggregation of silica.

There has been another report in the literature by Wilcoxon, Martin, and Schaefer[48] claiming that colloidal gold can not be aggregated by RLCA. This was based on a measurement of the kinetics determined from the time dependence of the apparent hydrodynamic radius $\bar{R}_{\rm eff} = q^2\zeta/\Gamma_1$, calculated directly from the first cumulant. This $\bar{R}_{\rm eff}$ was found to be linear in time rather than exponential, and the fractal dimension of the clusters produced was $d_f \approx 1.8$. The problem with the results of Wilcoxon, Martin, and Schaefer is actually trivial, and is immediately apparent when the aggregation rate they report is compared with other measurements of reaction-limited colloid aggregation. They used an initial concentration that was a factor of 10 less than that used in the present work. Nevertheless, at $t_a = 100$ min, they reported $\bar{R}_{\rm eff} \approx 200$ nm. By comparison, a similar measurement of $\bar{R}_{\rm eff}$ for true RLCA, using a colloid with an initial concentration a factor of 10 higher, does not reach $\bar{R}_{\rm eff} \approx 200$ nm until $t_a \approx 450$ min, a factor of nearly 5 larger than the lower concentration results reported by Wilcoxon, Martin, and Schaefer. Thus their results are simply not in the limit of RLCA regime. Instead, their results reflect the crossover behavior in the intermediate regime, which has been previously reported.[11] This behavior occurs when the aggregation rate is slower than the diffusion limit and, as such, behaves as reaction-limited aggregation. However, as the number of cluster decreases due to the aggregation, diffusion becomes increasingly important in determining the rate limiting step, and thus the aggregation must ultimately pass over to DLCA. This aggregation is well described as a crossover behavior between reaction- and diffusion-limited colloid aggregation, and the kinetics can be qualitatively described as being initially exponential, then crossing over to the power-law behavior characteristic of DLCA. However, these kinetics can often appear essentially linear in time, as shown in a

previous report for the kinetics of colloidal gold.[11] Thus the results of Wilcoxon, Martin, and Schaefer are simply not in the RLCA regime and the suggestion by the authors that RLCA gold results in linear kinetics is incorrect. We note, by contrast, that in obtaining the results reported in this paper, we ensure that the initial aggregation rate is sufficiently small that the crossover to DLCA is never approached in the course of our experiments, allowing us to study the true RLCA regime.

The work of Wilcoxon, Martin, and Schaefer also suggested that multiple scattering affected both the static and dynamic light scattering results for colloidal gold. However, the light scattering intensity from the colloidal silica is about three orders of magnitude less than from the gold. Nevertheless, we have shown here that both the static and dynamic results from the gold are *identical* to those from the much more weakly scattering silica. This is clear experimental evidence that multiple scattering does not affect the gold results. Moreover, detailed theoretical calculations demonstrate how the consequences of the fractal correlations persist, leading to the characteristic q^{-d_f} dependence of the static scattering, even in the presence of the optical resonance characteristic of metallic scatterers.[49]

Finally, there are reports of slow, and apparently reaction-limited colloid aggregation which clearly do not fall into the universal description presented in this paper. These entail the aggregation of biological molecules or proteins.[50,51] While their kinetics seem to be quite slow, in accord with the RLCA results presented here, the fractal dimension of the clusters produced is $d_f \approx 2.5$, consistently much higher than that measured here. A proposed explanation for this discrepancy is restructuring of the colloids which may occur due to the lower rigidity of the biological molecules compared to the colloids studied here. It is also possible that bonds formed are slightly weaker, effectively resulting in some annealing of the structures of the clusters. Either of these effects would be expected to increase the fractal dimension of the aggregates, consistent with the observation. However, whatever the cause, it is clear that a necessary condition for the universal RLCA behavior reported here is that the aggregation be truly irreversible and the aggregates formed be rigid.

VIII. CONCLUSIONS

In this paper, the process of reaction-limited colloid aggregation is studied using static and dynamic light scattering and a self-consistent description of the two forms of light scattering from colloidal aggregates is presented. Static light scattering is used to measure the fractal dimension of the clusters, as well as their structure factor. By assuming a power-law form for the cluster-mass distribution, we can also determine the cutoff mass of the clusters in the distribution, provided the aggregates are small enough so that $qR \sim 1$. This same distribution and cutoff mass can be used to describe the shape of the autocorrelation function measured by dynamic light scattering, provided the effects of rotational diffusion are included. Excellent agreement is obtained with the measurements. We also measure the ratio of the hydrodynamic radius to the radius of gyration of individual clusters, and find $\beta = 1.0$ for RLCA aggregates.

We study the effects of the power-law cluster-mass distribution on the behavior of dynamic light scattering, and show that it causes the results to be sensitive to clusters of all sizes. It leads to a q dependence of the first cumulant of the autocorrelation function, but we show that this cannot be simply expressed as $\Gamma_1 \sim q^{2+\alpha}$. Instead, the shape of the function $\bar{D}_{\text{eff}}(q) = \Gamma_1/q^2$, depends critically on several key features of the aggregation process: the distribution exponent τ, the effects of rotational diffusion, and the shape of the structure factor. We scale the measured data onto a single master curve, whose shape reflects the q dependence of $\bar{D}_{\text{eff}}$, obtaining the aggregation kinetics from this scaling. The shape of the master curve allows us to unambiguously determine the value of exponent for the cluster-mass distribution.

Since the shape of the master curve is so sensitive to the key features of the aggregation process, it can be used to critically compare the behavior of the aggregation of completely different colloids. We show that the master curves obtained from three completely different colloids, gold, silica, and polystyrene, are indistinguishable. This implies that the cluster-mass distribution, the structure of the clusters, and their anisotropy are identical for each of the colloids. The cluster-mass distribution exponent is $\tau = 1.5 \pm 0.05$ for each colloid. In addition, the aggregation kinetics for each colloid exhibit exponential growth. Finally, the fractal dimensions measured by static light scattering are $d_f = 2.1 \pm 0.05$ and are identical for each colloid. These are in good agreement with the theoretical predictions of the RLCA model. Thus the results presented here provide striking confirmation that reaction-limited colloid aggregation is a universal process.

---

*Present address: National Institute of Standards and Technology, React A106, Gaithersburg, MD 20899.

[1]P. Meakin, in *Phase Transitions and Critical Phenomena,* edited by C. Domb and J. L. Lebowitz (Academic, New York, 1988), Vol. 12, p. 335.

[2]*Kinetic Aggregation and Gelation,* edited by F. Family and D. P. Landau (Elsevier, Amsterdam, 1984).

[3]D. A. Weitz, M. Y. Lin, and J. S. Huang, in *Physics of Complex and Supermolecular Fluids,* edited by S. A. Safran and N. A. Clark (Wiley-Interscience, New York, 1987), p. 509.

[4]D. A. Weitz and M. Oliveria, Phys. Rev. Lett. **52**, 1433 (1984).

[5]M. Y. Lin, H. M. Lindsay, D. A. Weitz, R. C. Ball, R. Klein, and P. Meakin, Proc. R. Soc. London Ser. A **423**, 71 (1989).

[6]M. Y. Lin, H. M. Lindsay, D. A. Weitz, R. C. Ball, R. Klein, and P. Meakin, Nature **339**, 360 (1989).

[7]E. J. W. Verwey and J. T. G. Overbeek, *Theory of the Stability of Lyophobic Colloids* (Elsevier, Amsterdam, 1948).

[8]R. C. Ball, D. A. Weitz, T. A. Witten, and F. Layvraz, Phys.

Rev. Lett. **58**, 274 (1985).
[9]B. B. Mandelbrot, *The Fractal Geometry of Nature* (Freeman, San Franciso, 1982).
[10]D. W. Schaefer, J. E. Martin, P. Wiltzius, and D. S. Cannell, Phys. Rev. Lett. **52**, 2371 (1984).
[11]D. A. Weitz, J. S. Huang, M. Y. Lin, and J. Sung, Phys. Rev. Lett. **54**, 1416 (1985).
[12]G. K. Von Schultess, B. G. Benedek, and R. W. de Blois, Macromolecules **13**, 939 (1980).
[13]M. Matsushita, Y. Hayakawa, K. Sumida, and Y. Sawada, in *Proceedings of the First International Conference for Science on Form, Tokyo, 1986,* edited by S. Ishizaka (KTK Scientific, Tokyo, 1986), p. 23.
[14]P. N. Pusey and J. G. Rarity, Mol. Phys. **62**, 411 (1987).
[15]J. G. Rarity, R. N. Seabrook, and R. J. G. Carr, Proc. R. Soc. London Ser. A **423**, 89 (1989).
[16]J. S. Huang, J. Sung, M. Eisner, S. C. Moss, and J. Gallas, J. Chem. Phys. **90**, 25 (1989).
[17]P. Dimon, S. K. Sinha, D. A. Weitz, C. R. Safinya, G. S. Smith, W. A. Varady, and H. M. Lindsay, Phys. Rev. Lett. **57**, 595 (1986).
[18]W. D. Brown and R. C. Ball, J. Phys. A **18**, L517 (1985).
[19]R. Jullien and M. Kolb, J. Phys. A **17**, L639 (1984).
[20]P. Meakin, Adv. Colloid Interface Sci. **28**, 249 (1988).
[21]H. M. Lindsay, R. Klein, D. A. Weitz, M. Y. Lin, and P. Meakin, Phys. Rev. A **39**, 3112 (1989).
[22]R. J. Cohen and G. B. Benedek, J. Phys. Chem. **86**, 3696 (1982).
[23]G. J. Von Dongen and M. H. Ernst, Phys. Rev. Lett. **54**, 1396 (1985).
[24]T. Vicsek and F. Family, Phys. Rev. Lett. **52**, 1669 (1984).
[25]P. Meakin and F. Family, Phys. Rev. A **36**, 5498 (1987).
[26]M. S. Bowen, M. L. Broide, and R. J. Cohen, in Ref. 2, p. 185.
[27]M. L. Broide, Ph.D. thesis, Massachusetts Institute of Technology, 1988.
[28]J. E. Martin and D. W. Schaefer, Phys. Rev. Lett. **53**, 2457 (1984).
[29]J. E. Martin, Phys. Rev. A **36**, 3415 (1987).
[30]J. E. Martin and F. Leyvraz, Phys. Rev. A **34**, 2346 (1986).
[31]D. A. Weitz and M. Y. Lin, Phys. Rev. Lett. **57**, 2037 (1986).
[32]D. S. Cannell and C. Aubert, in *On Growth and Form,* edited by H. E. Stanley and N. Ostrowskey (Nijhoff, Dordrecht, 1986), p. 187.
[33]P. N. Pusey, in *Photon Correlation Spectroscopy and Velocimetry,* edited by H. Z. Cummins and E. R. Pike (Plenum, New York, 1976), p. 45.
[34]B. J. Berne and R. Pecora, *Dynamic Light Scattering* (Wiley, New York, 1976).
[35]E. Y. Sheu, S. H. Chen, and J. S. Huang, J. Phys. Chem. **91**, 1535 (1987).
[36]J. Turkevich, P. C. Stevenson, and J. Hillier, Trans. Discuss. Faraday Soc. **11**, 55 (1951).
[37]R. Buscall, P. D. A. Mills, J. W. Goodwin, and D. W. Lawson, J. Chem. Soc. Faraday Trans. **1**, 4249 (1988).
[38]D. A. Weitz and M. Y. Lin, in *NASA Laser Light Scattering Advanced Technology Development Workshop, Cleveland, 1988,* edited by W. V. Meyer (NASA, Washington, D.C., 1989), p. 173.
[39]H. M. Lindsay, M. Y. Lin, D. A. Weitz, R. C. Ball, R. Klein, and P. Meakin, in *Proceedings of the Photon Correlation Techniques and Applications, Washington, D.C., 1988,* edited by J. B. Abbiss and A. E. Smart (Optical Society of America, Washington, D.C., 1988), Vol. 1, p. 122.
[40]M. Y. Lin, R. Klein, H. M. Lindsay, D. A. Weitz, R. C. Ball, and P. Meakin, J. Colloid Interface Sci. (to be published).
[41]H. M. Lindsay, R. Klein, D. A. Weitz, M. Y. Lin, and P. Meakin, Phys. Rev. A **38**, 2614 (1988).
[42]R. C. Ball, H. M. Lindsay, D. A. Weitz, and M. Y. Lin (unpublished).
[43]Z.-Y. Chen, P. Meakin, and J. M. Deutch, Phys. Rev. Lett. **59**, 2121 (1987).
[44]W. Hess, H. L. Frisch, and R. Klein, Z. Phys. B **64**, 65 (1986).
[45]P. Wiltzius, Phys. Rev. Lett. **58**, 710 (1987).
[46]P. N. Pusey, J. G. Rarity, R. Klein, and D. A. Weitz, Phys. Rev. Lett. **59**, 2122 (1987).
[47]M. Y. Lin, H. M. Lindsay, D. A. Weitz, R. Klein, R. C. Ball, and P. Meakin, J. Phys. Condens. Matter (to be published).
[48]J. P. Wilcoxon, J. E. Martin, and D. W. Schaefer, Phys. Rev. A **39**, 2675 (1989).
[49]Z. Chen, P. Sheng, D. A. Weitz, H. M. Lindsay, and M. Y. Lin, Phys. Rev. B **37**, 5232 (1988).
[50]J. Feder, T. Jossang, and E. Roenqvist, Phys. Rev. Lett. **53**, 1403 (1984).
[51]D. S. Horne, Faraday Discuss. Chem. Soc. **83**, 259 (1987).